Natural-resistance-associated macrophage protein 1 is an H^+/bivalent cation antiporter

Tapasree GOSWAMI*, Arin BHATTACHARJEE†, Paul BABAL‡, Susan SEARLE*, Elizabeth MOORE§, Ming LI† and Jenefer M. BLACKWELL*[1]

*Wellcome Trust Centre for Molecular Mechanisms in Disease, Wellcome Trust/MRC Building, Addenbrooke's Hospital, Hills Road, Cambridge CB2 2XY, U.K., †Department of Pharmacology, University of South Alabama College of Medicine, Mobile 36688, Alabama, U.S.A., ‡Department of Pathology, University of South Alabama College of Medicine, Mobile 36688, Alabama, U.S.A., and §U.S.A. Cancer Centre, University of South Alabama College of Medicine, Mobile 36688, Alabama, U.S.A.

In mammals, natural-resistance-associated macrophage protein 1 (Nramp1) regulates macrophage activation and is associated with infectious and autoimmune diseases. Nramp2 is associated with anaemia. Both belong to a highly conserved eukaryote/prokaryote protein family. We used *Xenopus* oocytes to demonstrate that, like Nramp2, Nramp1 is a bivalent cation (Fe^{2+}, Zn^{2+} and Mn^{2+}) transporter. Strikingly, however, where Nramp2 is a symporter of H^+ and metal ions, Nramp1 is a highly pH-dependent antiporter that fluxes metal ions in either direction against a proton gradient. At pH 9.0, oocytes injected with cRNA from wild-type murine Nramp1 with a glycine residue at position 169 ($Nramp1^{G169}$; $P = 3.22 \times 10^{-6}$) and human NRAMP1 ($P = 3.87 \times 10^{-5}$) showed significantly enhanced uptake of radiolabelled Zn^{2+} compared with water-injected controls. At pH 5.5, $Nramp1^{G169}$ ($P = 1.34 \times 10^{-13}$) and NRAMP1 ($P = 1.09 \times 10^{-6}$) oocytes showed significant efflux of Zn^{2+}. Zn^{2+} transport was abolished when the proton gradient was dissipated using carbonyl cyanide *p*-trifluoromethoxyphenylhydrazone. Using pre-acidified oocytes, currents of 130 ± 57 nA were evoked by 100 μM Zn^{2+} at pH 7.5, and 139 ± 47 nA by 100 μM Fe^{2+} at pH 7.0, in $Nramp1^{G169}$ oocytes; currents of 254 ± 49 nA and 242 ± 26 nA were evoked, respectively, in NRAMP1 oocytes. Steady-state currents evoked by increasing concentrations of Zn^{2+} were saturable, with apparent affinity constants of approx. 614 nM for $Nramp1^{G169}$ and approx. 562 nM for NRAMP1 oocytes, and a curvilinear voltage dependence of transporter activity (i.e. the data points approximate to a curve that approaches a linear asymptote). In the present study we propose a new model for metal ion homoeostasis in macrophages. Under normal physiological conditions, Nramp2, localized to early endosomal membranes, delivers extracellularly acquired bivalent cations into the cytosol. Nramp1, localized to late endosomal/lysosomal membranes, delivers bivalent cations from the cytosol into this acidic compartment where they may directly affect antimicrobial activity.

Key words: metal-ion transporter, Nramp1, infection.

INTRODUCTION

In mammals, the natural-resistance-associated macrophage protein 1 (Nramp1) regulates macrophage activation and antimicrobial activity (reviewed in [1,2]), and is associated with infectious [3,4] and autoimmune [5–7] disease susceptibility. It localizes to membranes of the late endosomes/lysosomes of macrophages [8,9]. Its amino acid sequence predicts a protein with 10 or 12 putative membrane-spanning domains and a conserved transport motif [10,11], but its precise mode of action as a transporter has not been demonstrated.

Since the original cloning of *Nramp*1 [10], sequence analyses have identified a large family of Nramp-related proteins spanning eukaryotes and prokaryotes [11,12]. In yeast, the Nramp1 orthologue SMF1 (where SMF1 = suppressor of the mitochondrial import function mutation 1) is involved in high affinity Mn^{2+} uptake that is inhibited by Zn^{2+} [13]. Similarly, Mn^{2+} and Fe^{2+} ions suppress the abnormal taste behaviour of the mutant *malvolio* [14], the gene encoding the *Drosophila melanogaster* Nramp1 orthologue [15]. This effect is again inhibited by $ZnCl_2$. In mammals, Nramp2 controls anaemia [16] and has broad metal ion specificity including Fe^{2+}, Zn^{2+}, Co^{2+}, Cd^{2+}, Cu^{2+}, Ni^{2+} and Pb^{2+} [17]. Of these, Fe^{2+}, Zn^{2+} and Mn^{2+} are of specific interest as candidate metal ions contributing to the many pleiotropic effects ascribed to Nramp1 in regulating macrophage activation (reviewed in [1,2]). The redox-active Fe^{2+} metal ion, in particular, is of interest for its potential role in the direct generation of toxic antimicrobial hydroxyl radicals within the phagolysosomes of infected macrophages [18]. Zn^{2+} has also been shown to be important in directing endosomal fusion events [19], known to be defective in Nramp1 mutant macrophages infected with *Mycobacterium bovis* or *M. avium* [9,20,21]. In addition, it has been proposed that the influence of Nramp1 on lipopolysaccharide-dependent processing of antigen for presentation to T cells may be the result of failure to deliver essential ions for metalloprotease activity into the late endosomal major histocompatibility complex class II compartment [22]. In the present study we use the *Xenopus* oocyte model to analyse the role of Nramp1 in bivalent cation transport, and to characterize the transport function.

EXPERIMENTAL

Preparation of expression constructs

Full-length wild-type murine Nramp1 with a glycine residue at position 169 ($Nramp1^{G169}$) clone λ8.1 was originally isolated

Abbreviations used: FCCP, carbonyl cyanide *p*-trifluoromethoxyphenylhydrazone; Nramp1, natural-resistance-associated macrophage protein 1; $Nramp1^{G169}$, wild-type murine Nramp1 with a glycine residue at position 169; $Nramp1^{D169}$, murine Nramp1 with an aspartic acid residue at position 169; $NRAMP1^{CH}$, chimaeric Nramp1/NRAMP1 construct; pH_i, intracellular pH; RT–PCR, reverse-transcriptase–PCR; SMF1, suppressor of the mitochondrial import function mutation 1.

[1] To whom correspondence should be addressed (e-mail jennie.blackwell@cimr.cam.ac.uk).

from an activated murine macrophage cDNA library and engineered [23] to generate a clone of murine Nramp1 with an aspartic acid residue at position 169 (Nramp1^{D169}) equivalent to the mutant infectious-disease susceptible allele. To facilitate immunocytochemical localization, Nramp1^{G169} and Nramp1^{D169} were amplified by PCR using Bio-X-act DNA polymerase (Bioline, London, U.K.) from pBABE constructs used in a previous study [23] with primers (5′-TCGCTGACGTTTGATGATTAGTAGTGACAAGAGC-3′ and 5′-TTGATGGCGGCCGCTCACTTGTCATCGTCGTCCTTGTAGTCCGCTGCGGCCCCGGAACCCTGCAC-3′) designed to incorporate an 8-amino-acid FLAG epitope (i.e. Asp-Tyr-Lys-Asp-Asp-Asp-Asp-Lys) at the C-terminal end of the encoded protein. The resulting 1709 bp DNA fragments were TA-cloned into the vector pCRII (Invitrogen, Groningen, The Netherlands) and subcloned using *Eco*RV and *Bam*HI into the *in vitro* transcription vector pSP73 (Promega, Chilworth, Southampton, U.K.). The FLAG-containing Nramp1^{G169} pCRII clone was further modified to produce a chimaeric Nramp1/NRAMP1 construct (NRAMP1^{CH}) in which nucleotides encoding amino acids 66–418 (transmembrane domains 1–9; exons 3–12; incorporating the highly conserved transport motif) of the mouse sequence were replaced by the homologous region of the human cDNA, prior to subcloning into pSP73. A full-length human NRAMP1 cDNA construct was prepared using a nested reverse-transcriptase–PCR (RT–PCR) cloning strategy. Total RNA, isolated from the mature human monocytic cell line THP1 using TRIZOL reagent (Gibco BRL, Paisley, Renfrewshire, Scotland, U.K.), was used in a one-step RT–PCR reaction (Superscript One-step RT–PCR System, Gibco BRL) with primers located immediately 5′ (5′-GATGTAAGAGGCAGGGCAC-3′) and 3′ (5′-CAGATGAGGACACTGAGACC-3′) of the NRAMP1 coding region. The 1991 bp PCR product was then reamplified by PCR with Bio-X-act DNA polymerase using primers specific for the coding region and containing the sequence for a C-terminal FLAG epitope as in the above constructs (5′-TCGCTGACGCGTTTGATGACAGGTGACAAGGGTCC-3′ and 5′-TTGATGGCGGCCGCCTACTTGTCATCGTCGTCCTTGTAGTCCGCTGCGGCGCCAGAGGTCTCCCC-3′). The 1715 bp full-length human cDNA fragment was then TA-cloned into the pCRII vector. The integrity of all Nramp1/NRAMP1 cloned constructs used in the present study was confirmed by restriction-enzyme analysis and full-length double-stranded sequence analysis.

In vitro transcription

The murine and chimaeric pSP73 constructs were linearized using *Ssp*I and *Hpa*I to give 4142 bp of cDNA-containing fragments. The human NRAMP1 construct was linearized with *Bss*HII. Each DNA (1 μg) was then transcribed *in vitro* using SP6 or T7 (for pSP73 or pCRII constructs respectively) mMessage mMachine kits (Ambion, Austin, TX, U.S.A.). The quality of the cRNA obtained was confirmed by electrophoresis on a 1.9 % (w/v) formaldehyde/1.2 % (w/v) agarose gel, and cRNA was quantified by spectrophotometric analysis.

Collection and preparation of oocytes

Adult female *Xenopus laevis* were maintained in deionized water at room temperature (18–24 °C). Frogs were anaesthetized on ice and oocytes were collected using a sterile surgical technique. Oocytes were transferred to, and washed thoroughly in, calcium-free OR-2 medium [5 mM Hepes/NaOH (pH 7.5), 82.5 mM NaCl, 2 mM KCl and 1 mM $MgCl_2$]. Oocytes were defolliculated manually and enzymically by incubation with collagenase (1.5 mg/ml) at 20 °C for 2 h. Oocytes were washed extensively (seven to eight times) with OR-2 solution before transfer into L-15 growth medium [50 % (w/v) Leibovitz's L-15 medium, 5 % (w/v) heat-inactivated horse serum, 25 units/ml penicillin, 25 μg/ml streptomycin and 15 mM Hepes (pH 7.4)] in 24-well tissue culture plates and incubation on a slow speed rotator at 18 °C.

Injection of oocytes

Stage IV–stage VI oocytes were selected, and cytoplasmic injections were carried out with 50 nl of Nramp1^{G169}, Nramp1^{D169}, NRAMP1^{CH} or NRAMP1 cRNA (0.5 μg/μl), or water (control). Injected eggs were maintained individually in Eppendorf tubes with L-15 growth medium at 18 °C. The oocytes were washed extensively to remove antibiotic and metal ions present in the growth medium before electrophysiology or radiotracer uptake assays were performed.

Radiotracer uptake assay

Radioisotope transport was measured 4–5 days post-injection using $^{59}Fe^{2+}$, $^{59}Fe^{3+}$, $^{65}Zn^{2+}$ and $^{54}Mn^{2+}$ isotopes (DuPont NEN, Boston, MA, U.S.A.). Single oocytes, or pools of ten oocytes, were added to Eppendorf tubes, washed three times with OR-2 solution and washed once in incubation solution [96 mM NaCl, 2 mM KCl, 100 nM $CaCl_2$, 1 mM $MgCl_2$, 2.5 mM Hepes and either 2.5 mM Mes (pH 5.5 or pH 7.5) or 2.5 mM Ches (pH 9.0) buffered to pH 5.5, 7.5 or 9.0 with Tris]. Oocytes were incubated with isotope (10 μM) in incubation solution for 1–1.5 h at room temperature in a shaking water bath. The pH was measured after addition of the radioisotope, and the required pH was obtained and maintained using Mes or Ches, as appropriate. In the case of $^{59}Fe^{2+}$ assays, both the wash and incubation buffers contained 1 mM Ca^{2+} and 1×10^{-4} M ascorbate; the latter to keep the ferrous ion in its oxidation state of II. Oocytes were washed three times with incubation buffer containing 1 mM unlabelled bivalent cation, transferred to clean scintillation vials and radiotracer transport was determined using a scintillation counter.

The effect of dissipation of the electrochemical proton gradient across the oocyte membrane on $^{65}Zn^{2+}$ transport was measured similarly by including the protonophore carbonyl cyanide *p*-trifluoromethoxyphenylhydrazone (FCCP) at 2.5 μM in the incubation solution.

Electrophysiological measurements

Electrophysiological studies were carried out on oocytes 4–5 days post-injection using a two-microelectrode voltage clamp method. Oocytes were washed with recording solution (96 mM NaCl, 2 mM KCl, 100 nM $CaCl_2$, 1 mM $MgCl_2$, 100 μM ascorbic acid, 2.5 mM Hepes and 2.5 mM Mes, buffered to pH 5.5, 7.0 or 7.5 with Tris) and placed in a 0.15 ml perfusion chamber containing the same solution. Two standard glass microelectrodes (voltage and current electrodes respectively; 0.5–3 MΩ resistance) were filled with 3 M KCl and used to impale the oocyte and voltage clamp the oocyte membrane at a holding potential of -50 mV. Current was monitored continuously at a sampling frequency of 10 Hz using the X-Chart component of the HEKA Pulse + Pulse Fit software package (HEKA Electronik, Lambrecht, Germany). Oocytes were superfused continuously with recording solution in the presence or absence of substrate (100 μM), and the current was recorded over several minutes as indicated. The effect of adding bivalent cations was monitored over 1–2 min, and current reversal was

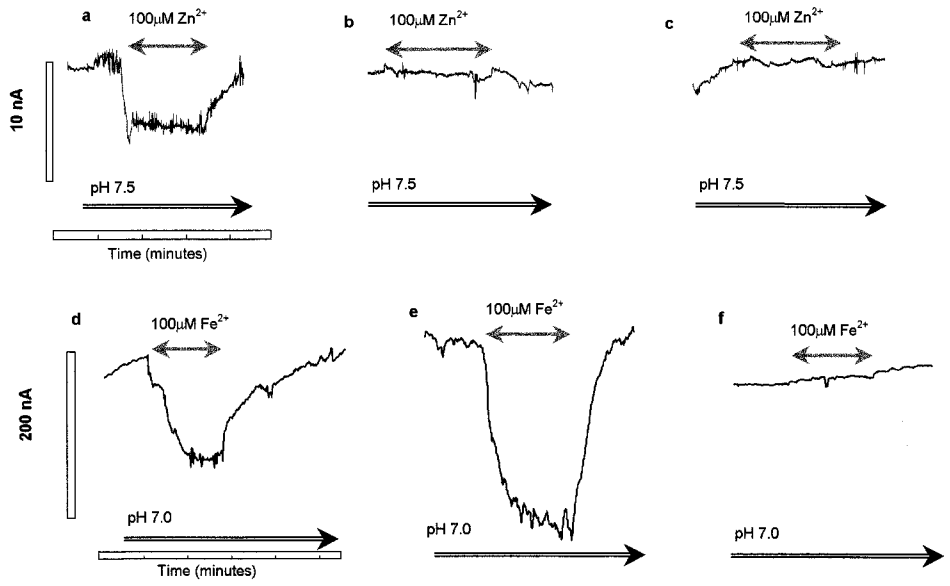

g

Treatment	Nramp1^{G169} Mean±SD	Nramp1^{G169} N oocytes	NRAMP1 Mean±SD	NRAMP1 N oocytes
100μM Zn^{2+}; pH 7.5	130±57 nA	5	254±49 nA	3
100μM Fe^{2+}; pH 7.0	139±47 nA	4	242±26 nA	5

Figure 1 Currents associated with the expression of Nramp1/NRAMP1 in oocytes

Current was continuously monitored in (**a**) Nramp1^{G169}-, (**b**) Nramp1^{D169}- and (**c**) water-injected (control) oocytes superfused with recording solution at pH 7.5. Current changes were recorded following the addition of 100 μM Zn^{2+} for 1–2 min, as indicated. Mn^{2+} (100 μM) evoked similar current changes in Nramp1^{G169}-injected oocytes at pH 7.5, but no rheogenic effects were observed for Fe^{2+} at pH 7.5, or for Fe^{2+}, Zn^{2+} or Mn^{2+} at pH 5.5. Larger currents were recorded in pre-acidified Nramp1^{G169}-injected (**d** and **g**) and NRAMP1-injected (**e** and **g**), but not water-injected (**f**), oocytes in response to 100 μM Fe^{2+} superfused at pH 7.0 or 100 μM Zn^{2+} superfused at pH 7.5.

observed by replacement with substrate-free recording solution. The apparatus allowed for the complete replacement of superfusion solution without a change in volume in the recording chamber. For some experiments, oocytes were pre-acidified by incubation in acetate buffer [60 mM NaCl, 5 mM KCl, 1 mM $MgCl_2$, 100 μM $CaCl_2$, 5 mM Hepes, 5 mM Mes and 30 mM sodium acetate (pH 6.0)] for 15 min at room temperature prior to superfusion with solutions at pH 7.0 (Fe^{2+}) or pH 7.5 (Zn^{2+}).

To analyse steady-state kinetics, current traces obtained with increasing concentrations of Zn^{2+} (0 nM, 10 nM, 100 nM, 1 μM, 10 μM and 100 μM) were fitted to the Michaelis–Menten equation:

$$I = I_{max} \cdot S/(K^S_{0.5} + S)$$

where I is the evoked current (i.e. the difference in steady-state current measured in the presence or absence of substrate), I_{max} is the derived current maximum, S is the substrate concentration and $K^S_{0.5}$ is the substrate concentration at which current is half-maximal. The voltage dependence of Zn^{2+}-evoked current was studied by applying step changes in the membrane potential of the clamped oocyte from -50 to -120 mV in 10 mV increments, for 30 s at each voltage, during superfusion with 100 μM Zn^{2+} at pH 7.5. Intracellular pH (pH_i) changes associated with Nramp1/NRAMP1-mediated bivalent cation transport in oocytes were monitored using pH-sensitive microelectrodes. Borosilicate pipettes were sialinized, back filled with 3 M KCl and their tips filled with an H^+-selective ionophore (Fluka, Gillingham, Dorset, U.K.; ionophore II, cocktail A). Following calibration of the pH electrode, the electrode was used to measure the pH_i of the acidified oocytes and pH changes during superfusion with recording solution at pH 7.5 in the presence and absence of 100 μM Zn^{2+}.

Immunocytochemistry

Expression of Nramp1^{G169} and Nramp1^{D169} proteins was examined in 4–5-day post-injection oocytes. Oocytes (5–10) were snap frozen in Tissue-Tek (Miles Inc., Pittsburgh, PA, U.S.A.), cryosectioned, and the sections were mounted on to glass slides. Sections were incubated for 10 min with 0.05% hydrogen peroxide in 95% (v/v) ethanol, for 1 h with FLAG-M2 mouse monoclonal IgG antibody (Sigma; 10 μg/ml) in PBS containing 5% (w/v) BSA, and for 30 min with rabbit anti-mouse, peroxidase-conjugated, IgG (DAKO peroxidase envision system; DAKO, Serastopol, Ukraine). The sections were subsequently treated with the DAKO peroxidase reaction chromagen, aminoethylcarbazole, until red staining was visualized using an inverted light microscope. All incubations were carried out at room temperature, and interspersed with a 5 min wash in PBS containing 5% BSA. Sections were mounted in glycerol/gelatin (DAKO) and examined using high-power light microscopy.

Immuno-electronmicroscopy

Expression of Nramp1/NRAMP1 proteins was also investigated in 4–5-day post-injection oocytes using immuno-electron-

microscopy. Oocytes were fixed for 24 h in cold 3% (w/v) glutaraldehyde in 0.2 M cacodylate buffer (pH 7.2), washed three times for 30 min in 0.1 M cacodylate buffer, two times in 70% ethanol, and placed in water-based LR White Embedding Medium (Ted Pella, Inc., Redding, CA, U.S.A.) at 4 °C for 2 h. This process was repeated two times before oocytes were transferred to a gelatin capsule and covered with embedding medium, which was polymerized for 48 h at 55 °C. Sections (80 nm) were cut using an ultramicrotome and mounted on to separate nickel grids. For immuno-gold labelling, grids were treated with PBS (pH 7.2) for 10 min, blocked for 30 min in PBS containing 1% BSA, and incubated for 2 h at room temperature with FLAG-M2 mouse monoclonal antibody (Sigma; 10 μg/ml) in PBS containing 0.5% BSA and 0.005% Tween. Grids were washed three times for 15 min in buffer, incubated for 1 h with second layer anti-(mouse-IgG) 10 nm colloidal gold (Sigma; 1:450 dilution), and washed three times for 10 min in buffer and once in filtered water. Sections were counterstained with lead citrate and uranyl acetate and examined in a Phillips CM 100 transmission electron microscope at 80 kV. Control grids were prepared omitting the primary antibody.

RESULTS

Currents in Nramp1-expressing *Xenopus* oocytes

Initial two-microelectrode voltage clamp analysis of oocytes injected with cRNA evoked small, but reproducible and reversible, inward currents of approx. 7 nA for Nramp1^{G169} (Figure 1a) and approx. 10 nA for NRAMP1^{CH} (results not shown) when oocytes were clamped at a holding potential of -0 mV and superfused with 100 μM Zn^{2+} at pH 7.5. Similar results were obtained using 100 μM Mn^{2+} (results not shown), but currents could not be measured with Fe^{2+} at pH 7.5, because of the difficulty in maintaining iron in the ferrous valence state at this pH. No inward current was observed at pH 5.5 with 100 μM Zn^{2+}, Fe^{2+} or Mn^{2+} (results not shown). Nramp1^{D169}-injected or water-injected control oocytes clamped at a holding potential of -50 mV at pH 7.5 showed no significant rheogenic effects on addition of 100 μM Zn^{2+} (Figures 1b and 1c) or 100 μM Mn^{2+} (results not shown).

Transport is proton-coupled and antiport in nature

To further elucidate the role of pH in Nramp1-mediated transport of bivalent cations, transport of radiolabelled $^{65}Zn^{2+}$ was examined at extracellular pH values of 5.5, 7.5 and 9.0 in Nramp1^{G169}-, NRAMP1^{CH}- and NRAMP1-injected oocytes (Figure 2). At pH 9.0, there was reproducible net inward transport of Zn^{2+} using all three constructs. At pH 5.5 there was a striking net transport of Zn^{2+} out of oocytes (Figure 2a). Nramp1/NRAMP1 activity at pH 5.5 was therefore dependent on, and potentially limited by, the activity of an endogenous oocyte transporter responsible for the delivery of labelled cations into the oocyte. At pH 7.5 there was no net movement of Zn^{2+} across the oocyte membrane relative to the water-injected control in Nramp1^{G169}-injected oocytes. Oocytes injected with cRNA for the chimaeric NRAMP1^{CH} ($P = 0.022$) or full-length human NRAMP1 ($P = 3.1 \times 10^{-7}$), however, maintained significant net outward transport of Zn^{2+} relative to water-injected control oocytes. The activity of NRAMP1^{CH} at pH 7.5 was clearly less efficient than NRAMP1, indicating that the N-terminal region derived from murine Nramp1 may be involved in differential regulation of transport activity. Overall, these results confirm that bivalent cations are transported in the direction opposite to that of the H^+ gradient, i.e. antiport, rather than symport as demonstrated for Nramp2 [17], and that Nramp1 can flux metal ions in either direction depending on the pH gradient across the membrane.

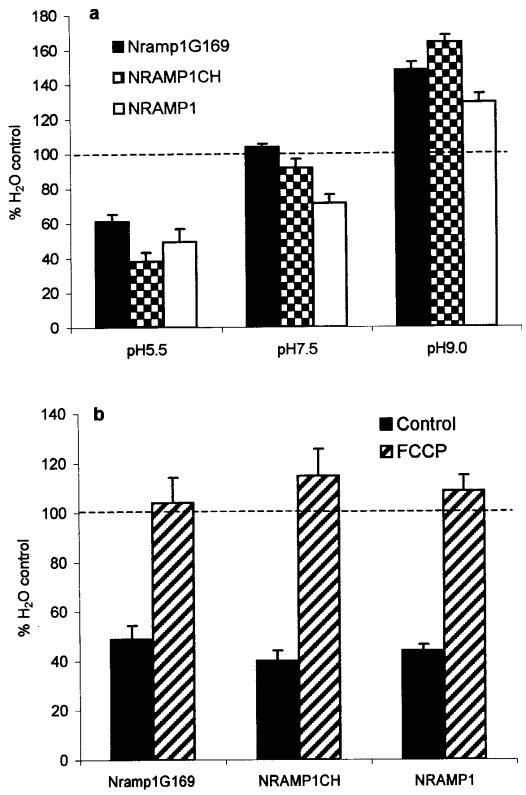

Figure 2 Nramp1/NRAMP1 transport is proton-coupled and is antiport in nature

(**a**) Effect of pH on radioactive $^{65}Zn^{2+}$ uptake in Nramp1^{G169}-, NRAMP1^{CH}- and NRAMP1-injected oocytes. Results are presented relative to water-injected controls. Student's *t* tests were performed using absolute counts. Data points are the means $\pm$ S.E.M. for 5–6 separate experiments in which radioactive uptake was measured in 3–5 individual oocytes/treatment for each experiment. At pH 5.5, Nramp1/NRAMP1 exports bivalent cations taken up by endogenous oocyte transporters. Differences in mean absolute counts for radioactivity were significant (2-tailed, unequal variance, Student's *t* test); $P = 1.35 \times 10^{-13}$ for water compared with Nramp1^{G169}, $P = 7.57 \times 10^{-31}$ for water compared with NRAMP1^{CH}, and $P = 1.09 \times 10^{-06}$ for water compared with NRAMP1-injected oocytes. NRAMP1 ($P = 3.10 \times 10^{-7}$ compared with water) and NRAMP1^{CH} ($P = 0.022$), but not Nramp1^{G169} (water compared with Nramp1^{G169} was not significant), retained some capacity to export Zn^{2+} at pH 7.5. At pH 9.0, Nramp1/NRAMP1 enhanced uptake of bivalent cations into oocytes ($P = 3.22 \times 10^{-6}$ for water compared with Nramp1^{G169}, $P = 1.73 \times 10^{-13}$ for water compared with NRAMP1^{CH}, and $P = 3.87 \times 10^{-5}$ for water compared with NRAMP1-injected oocytes). (**b**) FCCP, which dissipates the proton gradient across the oocyte membrane, neutralizes Nramp1^{G169}-, NRAMP1^{CH}-, and NRAMP1-mediated export of radioactive $^{65}Zn^{2+}$ from oocytes incubated at pH 5.5. This demonstrates that transport of Zn^{2+} is proton coupled. No significant differences in uptake of $^{65}Zn^{2+}$ were observed between water-injected or FCCP-treated water-injected oocytes over six independent experiments, demonstrating that FCCP did not affect the activity of the endogenous oocyte Zn^{2+} transporter.

Addition of the protonophore FCCP, which dissipates the electrochemical proton gradient across the membrane, completely neutralized Nramp1/NRAMP1-mediated transport of Zn^{2+} (Figure 2b). This experiment confirms that bivalent cation transport by Nramp1/NRAMP1 is proton coupled. The transport of bivalent cations and the directionality of this flux are energized and completely dependent on the presence of a transmembrane proton gradient.

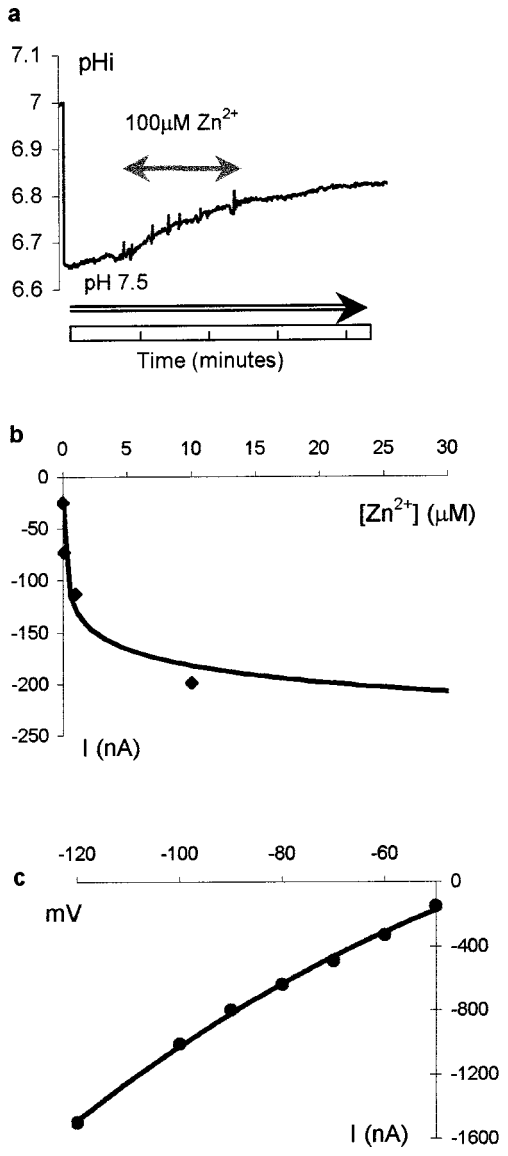

Figure 3 Characteristics of Zn^{2+} transport in oocytes

(**a**) pH_i was recorded in $Nramp1^{G169}$-injected oocytes during superfusion at pH 7.5 and addition of 100 μM Zn^{2+}. The pH electrode was calibrated to pH 7.0. (**b**) Concentration dependence of currents evoked by increasing concentrations of Zn^{2+} in NRAMP1-injected oocytes. (**c**) Voltage dependence of steady-state currents evoked by 100 μM Zn^{2+} in NRAMP1-injected oocytes with step-wise increases in voltage from -50 to -120 mV.

Currents evoked in pre-acidified oocytes

The demonstration that Nramp1/NRAMP1 is an antiporter suggested that stronger inward electrophysiological currents might be obtained by pre-acidifying the oocytes prior to clamping and superfusion at neutral or alkaline pH. This would also facilitate further characterization of the antiport activity, and allow direct demonstration that Fe^{2+} is a substrate for H^+ exchange. Under these conditions (Figures 1d–1g), currents of 130 ± 57 nA (mean $\pm$ S.D., $n = 5$) were evoked by 100 μM Zn^{2+} at pH 7.5 and 139 ± 47 nA ($n = 4$; see Figure 1d) by 100 μM Fe^{2+} at pH 7.0 in $Nramp1^{G169}$-injected oocytes. Currents of 254 ± 49 nA ($n = 3$) were evoked by 100 μM Zn^{2+} at pH 7.5 and 242 ± 26 nA ($n = 5$; see Figure 1e) by 100 μM Fe^{2+} at pH 7.0 in pre-acidified oocytes injected with human NRAMP1 cRNA. Neither cation evoked any significant currents in pre-acidified $Nramp1^{D169}$-injected oocytes (results not shown) or water-injected oocytes (see Figure 1f) clamped under the same conditions.

The effect of addition of Zn^{2+} on pH_i was recorded using pH-sensitive microelectrodes. Superfusion of clamped pre-acidified ($pH_i = 6.5 \pm 0.2$) oocytes with the recording solution at pH 7.5 resulted in a steady increase in pH_i, rapidly but reversibly enhanced by the addition and subsequent removal of Zn^{2+} (Figure 3a). That is, when Nramp1 is transporting Zn^{2+} into the oocyte, antiport of H^+ out of the oocyte causes a more rapid raise in pH_i. The biphasic response exhibited by $Nramp^{G169}$-injected oocytes was not observed in acidified water-injected control oocytes, where the rate of increase in pH_i was independent of and not affected by Zn^{2+} (results not shown). The Nramp1-mediated Zn^{2+}-coupled alkalinization and hence dissipation of the transmembrane proton gradient of acidified oocytes explain our separate observation that when reversible currents are evoked by repeated treatment with 100 μM Zn^{2+} and measured successively from the same oocyte, there is a gradual reduction in the magnitude of the successive inward currents generated (results not shown). In our experimental system, we were unable to simultaneously monitor pH_i and membrane potential in acidified oocytes, which would have allowed us to determine stoichiometry. Since orientation of Nramp1 in the oocyte membrane favoured efflux over influx of metal ions at low external pH, a more conventional measurement of stoichiometry by comparison of the initial rate of substrate uptake with substrate accumulation and flux in time course experiments would be confounded by the dependence of efflux on rates of uptake of metal ions into oocytes by endogenous transporters. Conditions under which Nramp1-mediated inward transport of metal ions could be measured, i.e. high external pH, would not provide the physiologically relevant direction of flux and would be confounded by the instability of bivalent cations at pH 9.0.

Steady-state currents evoked by increasing concentrations of Zn^{2+} were saturable (Figure 3b), with apparent affinity constants of approx. 614 nM for $Nramp1^{G169}$-injected oocytes and approx. 562 nM for NRAMP1-injected oocytes. Step-wise increases in voltage (-50 to -120 mV) following superfusion with 100 μM Zn^{2+} at pH 7.5 demonstrated a curvilinear voltage dependence of transporter activity in both $Nramp1^{G169}$-injected (results not shown) and NRAMP1-injected (Figure 3c) oocytes (i.e. the data points approximate to a curve that approaches a linear asymptote). The current/voltage (I/V) relationship supports the findings of both the electrophysiological and radioisotope data. At negative membrane potentials the inward flux of bivalent cations increased giving rise to measurable inward currents in oocytes clamped at -50 mV (Figures 1a–1e). Also, based on the I/V plot it appears that, as the membrane potential changes towards 0 mV, there is likely to be a voltage range between inward and outward current-inducing voltages in which there should be no significant bivalent cation evoked current at pH 7.5. This is demonstrated in the radioisotope data of Figure 2(a) where unclamped $Nramp^{G169}$ oocytes at pH 7.5 exhibited no significant inward or outward flux of bivalent cations.

Substrate specificity for bivalent cations

To determine substrate specificity for Nramp1-mediated metal-ion transport, further radioisotope assays were carried out using $^{59}Fe^{2+}$, $^{59}Fe^{3+}$, $^{65}Zn^{2+}$ and $^{54}Mn^{2+}$ (Figure 4). Ion selectivity studied under conditions favouring outward movement of bivalent cations confirmed net transport of Fe^{2+}, Zn^{2+} and Mn^{2+} out of $Nramp1^{G169}$-injected oocytes compared with water-injected

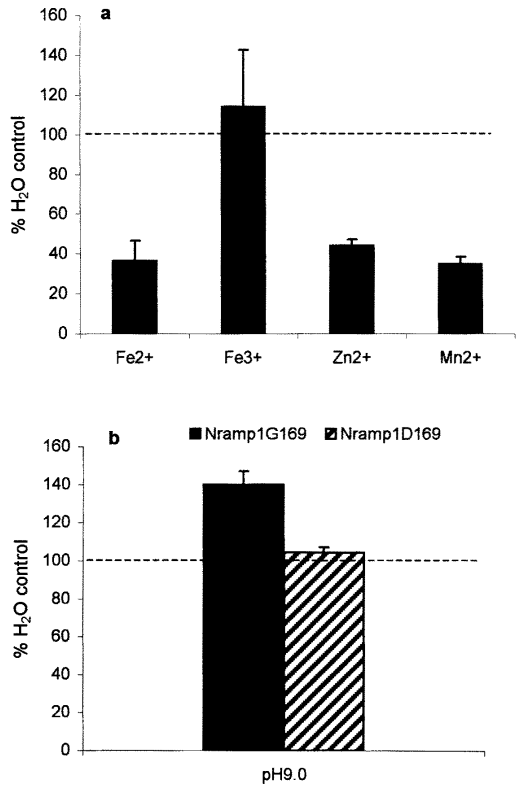

Figure 4 Selectivity of cation transport for wild-type, but not mutant, Nramp1

(**a**) Selectivity of Nramp1 for bivalent but not trivalent cation transport. Results are presented as means ± S.E.M. For four experiments (10 oocytes/tube per treatment for each experiment) in which Nramp1^{G169}- and water-injected oocytes were incubated for 1 h with $^{65}Fe^{2+}$, $^{59}Fe^{3+}$, $^{65}Zn^{2+}$ or $^{61}Mn^{2+}$ isotopes. Results are presented relative to water-injected controls. They confirm the efficiency with which the expressed Nramp1^{G169} protein exports bivalent cations from the oocyte, whereas Fe^{3+} shows no net inward/outward movement in transfected cells relative to water controls. Differences in absolute counts between water- and cRNA-injected oocytes are significant (2-tailed, unequal variance, Student's *t* test); $P = 0.07$ for Fe^{2+}, $P = 0.0006$ for Zn^{2+} and $P = 0.007$ for Mn^{2+}. (**b**) Nramp1^{D169}-injected oocytes fail to transport bivalent cations. Results are presented as means ± S.E.M. for four experiments in which $^{65}Zn^{2+}$ transport was measured in 3–5 individual oocytes/treatment in each experiment for Nramp1^{G169}-, Nramp1^{D169}- and water-injected oocytes incubated for 1 h with isotope at pH 9.0. Results are presented relative to water-injected controls. Differences in absolute counts between Nramp1^{G169}-injected oocytes compared with Nramp1^{D169}-injected oocytes are significant (2-tailed, unequal variance, Student's *t* test); $P = 1.20 \times 10^{-5}$. Absolute counts for Nramp1^{D169}-injected oocytes were not significantly different from water-injected oocytes.

controls, but showed no net inward or outward movement of Fe^{3+} (Figure 4a).

Effect of the Gly^{169} → Glu mutation on bivalent cation transport in the radioisotope assay

Under conditions favouring net inward transport of bivalent cations by Nramp1^{G169}-injected oocytes, Nramp1^{D169}-injected oocytes showed no significant inward or outward movement of Zn^{2+} relative to water-injected controls (Figure 4b).

Localization of Nramp1 in oocytes

Immunocytochemistry (Figure 5) using an antibody directed against the FLAG epitope engineered into the C-terminus of all Nramp1 constructs demonstrated that, whereas oocytes injected with Nramp1^{G169} cRNA showed clear localization of Nramp1 to the outer membrane of the oocyte (Figure 5a), FLAG-M2-specific staining in Nramp1^{D169}-injected oocytes was confined to the cytoplasm (Figure 5b). No staining was observed in water-injected control oocytes (Figure 5c). Analysis at the electron-microscope/immunogold level showed that NRAMP1^{CH} (Figure 5d), Nramp1^{G169} (Figure 5e) and NRAMP1 (results not shown) were localized to the microvilli [24] of the oocyte plasma membrane orientated with C-termini, and therefore by inference N-termini, on the cytoplasmic face of the membrane. Since Nramp1^{G169} constructs also contained a FLAG epitope, failure to localize Nramp1^{D169} to the oocyte plasma membrane appears not to be due to addition of the tag. It did mean, however, that we were unable to confirm whether the mutant Nramp1 molecule is completely defective in metal-ion transport function, or whether its reduced capacity to function in the mouse is due to fewer molecules reaching the membranes of late endosomes/lysosomes [8,9]. Previous electron-microscope/immunogold analysis [9] of primary bone-marrow-derived macrophages using specific anti-Nramp1 antibodies showed reduced expression of Nramp1^{D169} compared with Nramp1^{G169} on late endosomes and lysosomes, but provided no evidence for accumulation of mutant protein in any other intracellular compartments of mutant Nramp1^{D169} macrophages. Although differences in the stability of mutant compared with wild-type murine Nramp1 mRNA have been observed [18], studies with other Nramp family members [25,26] show that mutations also cause differences in protein stability and protein sorting for degradation.

DISCUSSION

Overall, our data show that Nramp1 is a highly pH-dependent bivalent cation transporter sharing substrate specificity with, but mechanistically different from, mammalian Nramp2. This mechanistic difference may account for the fact that, despite our and others' [27] demonstration that Nramp1 transports Mn^{2+}, Nramp2, but not Nramp1, can complement SMF1/SMF2 in yeast [28]. It may also explain why bivalent cation transport activity was measurable using the fluorescent metal-sensitive dye calcein in Nramp2 but not Nramp1 transfected Chinese hamster ovary cells [29], although localization of Nramp1 to the plasma membrane in this system was not confirmed as it was for Nramp2. Antiport versus symport activities are of interest when comparing mammalian Nramp1 and Nramp2 functions (Figure 6). Under physiological conditions, Nramp2 functions in the enterocytes lining the gut [17,30], specifically in early endosomal compartments [31,32], to transport metal ions from low (gut lumen or intravesicular) to high (cytoplasmic) pH. In constrast, in the normally acidic late endosomal/lysosomal compartment, Nramp1 will function to transport Fe^{2+} and other metal ions from high (cytoplasmic) to low (intravesicular) pH. Our model of Nramp1 function (Figure 6) differs from published models [32,33], both of which have interpreted Nramp1 function as symport by analogy with Nramp2. There are many examples where symport and antiport activities occur in different members of transport families where sequence conservation is high, even across transmembrane domains [34]. These include families where, like Nramp1/2, transport is not directly driven by ATP hydrolysis. In this case the energy for transport is provided by an electrochemical proton gradient (reviewed in [35]) which, for Nramp1 function, is maintained by the activity of the vesicular ATPase [21]. Interestingly, studies of other families of membrane transporters have shown that stoichiometry also remains the same despite subdivision of members of the same family into antiport and symport activities [36–38]. Hence, although we were unable to measure stoichiometry for Nramp1 in our experiments,

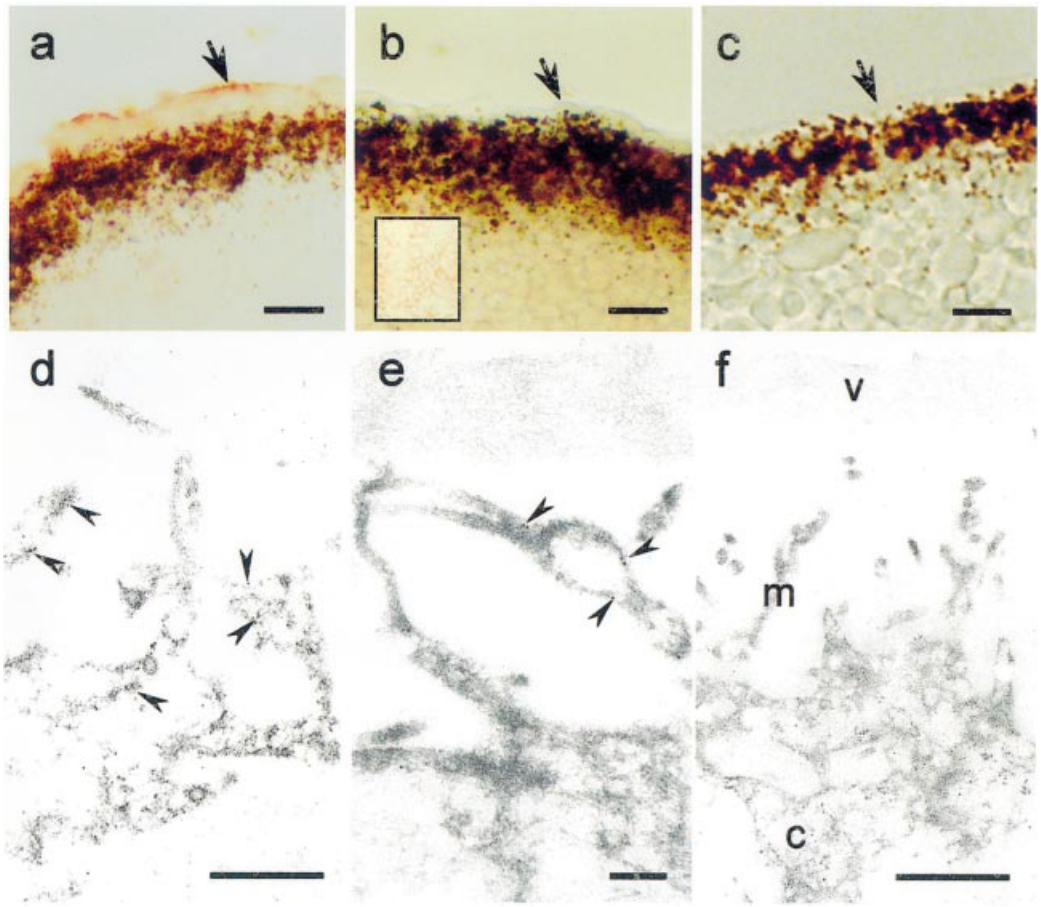

Figure 5 Immunocytochemical and electron-microscope/immunogold localization of Nramp1 in ooctyes

Immunocytochemistry demonstrating (**a**) FLAG-M2-specific staining at the plasma membrane in $Nramp1^{G169}$-injected oocytes, (**b**) no FLAG-M2-specific staining at the plasma membrane in $Nramp1^{D169}$-injected oocytes (the inset shows FLAG-M2-specific staining on inner membranes of the oocyte) and (**c**) no FLAG-M2-specific staining in a water-injected control oocyte. Arrows point to the plasma membrane in each case. Bars for (**a**, **b** and **c**) represent 1 μm. Immuno-gold labelling of electron microscope sections shows (**d**) FLAG-M2-specific staining on the micro-villi of the oocyte plasma membrane in a $NRAMP1^{CH}$-injected oocyte (bar = 500 nm), (**e**) gold labelling on the cytoplasmic face of the plasma membrane in a $Nramp1^{G169}$-injected oocyte (bar = 200 nm), and (**f**) no labelling in water-injected control oocytes (bar = 500 nm). Arrowheads indicate gold labelling. Abbreviations used: v, vitelline envelope; m, microvilli of plasma membrane; c, cytoplasm.

it is likely that this will have been conserved across family members, i.e. 1:1 bivalent cation/H^+ as for Nramp2 [17].

Previous attempts to define Nramp1 function using radioisotopes and fluid-phase or particle-bound bivalent-cation-sensitive fluorescent probes have produced contradictory results [18,27,39,40]. Atkinson and Barton [39] found that ectopic expression of Nramp1 was associated with reduced cellular iron loads, leading them to postulate that Nramp1 may be involved in a salvage pathway of iron recycling, but they did not specifically examine movement of iron across the late endosomal/lysosomal membrane. Kuhn et al. [40] found that there was no difference in the rate of Fe import or export between intact macrophages that had been stably transfected with wild-type $Nramp1^{G169}$ or mutant $Nramp1^{D169}$. However, the rate of ^{55}Fe import by latex-bead [40] or *M. avium* [18] phagosomes isolated from $Nramp1^{G169}$-transfected macrophages was more than double the rate by latex-bead or *M. avium* phagosomes from $Nramp1^{D169}$-transfected macrophages. Furthermore, phagosomes isolated from $Nramp1^{G169}$ macrophages pre-labelled with ^{55}Fe-citrate before phagocytosis contained up to 4-fold as much Fe as the corresponding phagosomes from $Nramp1^{D169}$ macrophages [40]. These results were consistent with the hypothesis that Nramp1 functions to transport Fe into phagosomes in the intact cell, as well as with the further observations of Zwilling et al. [18] that mycobacteria are killed by the generation of hydroxyl radicals via the Fenton and/or Haber–Weiss reactions in the phagosomes of macrophages from $Nramp1^{G169}$, but not $Nramp1^{D169}$, mice. Gomas and Appelberg [41] found, on the other hand, that an excess of iron delivered as iron-dextran to mice infected with *M. avium in vivo* interfered with $Nramp1^{G169}$ resistance. These authors believed that their data indicated that resistance was caused by iron starvation of the mycobacteria, that Nramp1 mediated iron export from phagosomes, and that iron overloading eventually saturated the ability of Nramp1 to deplete the phagosome of iron. Using a bivalent-cation-sensitive fluorescent probe covalently attached to zymosan particles, Jabado et al. [27] provided more direct evidence that phagosomes from $Nramp1^{G169}$ macrophages extrude Mn^{2+} faster than Nramp1-deficient macrophages, with the difference in rate of transport eliminated when acidification of the phagosomal lumen was dissipated. This was demonstrated by measuring the rate of quenching of particle-bound fluorescence following addition of exogenous 500 μM Mn^{2+}. Interestingly, the ability of Zwilling et al. [18] to inhibit mycobacterial growth in $Nramp1^{G169}$ macrophages by the addition of exogenous iron was dose-dependent, reaching a maximum at 0.05 μM iron and decreasing at higher concentrations,

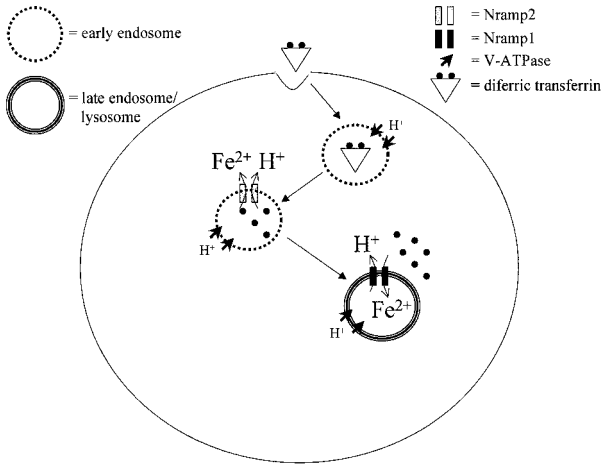

Figure 6 Model of bivalent cation homoeostasis in macrophages

The symport activity [17] of Nramp2 delivers bivalent cations (e.g. Fe^{2+}) to the cytosol across early endosomal membranes following recruitment of the vesicular ATPase (V-ATPase) and acidification of the vacuole [31]. The antiport activity of Nramp1 delivers bivalent cations from the cytosol to acidic late endosomes and lysosomes where the Fenton and/or Haber–Weiss reactions generate toxic antimicrobial radicals [18].

up to 0.5 μM. Our results in the present study demonstrating Nramp1 antiport activity are broadly consistent with the delivery of bivalent cations into acidic phagosomes under normal physiological conditions. It should be noted, however, that our data demonstrate that Nramp1 can flux bivalent cations in either direction depending on the pH on either side of the membrane. It is possible that viable pathogenic microbes may influence this process by altering phagosomal pH and/or bivalent cation concentrations. In the frog oocyte system we have not directly measured the influence of changing concentrations of bivalent cations on the direction of flux. Net flux will be determined by the combined electrochemical gradients of the metal ions and H^+, which may explain the discrepancies in results from different laboratories using different techniques and experimental conditions to evaluate the direction of transport across macrophage phagosomal membranes. More refined studies in the macrophage system will be required to further evaluate Nramp1 function, and the conditions under which influx compared with efflux from Nramp1-positive vesicles is observed.

Previous studies have shown that a variety of mammalian cell types, including macrophages, contain small amounts of redox-active iron in their lysosomes [42]. Exocytosis of lysosomal redox-active iron by macrophages is important for the oxidation and uptake of low-density lipoproteins [43]. In a separate study (V. Mulero, X.-q. Wei, F. Y. Liew, J. M. Blackwell, C. H. Barton and J. H. Brock, unpublished work) we have shown that Nramp1 regulates iron recycling when iron is presented to macrophages as immune complexes that target to late endosomal/lysosomal compartments, but not with transferrin-bound iron that targets only to the early endosomal compartment. Exocytosis of lysosomal redox-active iron by macrophages has been implicated as an early step in the formation of atheromatous lesions [44], thus extending the possible disease associations for which NRAMP1 should be examined. Foam cells in atherosclerotic lesions, which are derived from macrophages, were shown to contain heavy metals with a mainly lysosomal localization [44]. Monocyte-derived macrophages exposed to artificially aged erythrocytes showed an enhanced capacity to oxidize low-density lipoproteins due to exocytosed iron. Increases in the level of the lysosomal redox-active pool could predispose macrophages to oxidative stress. Garner et al. [42] demonstrate that exposure of macrophages to oxidative stress (hydrogen peroxide) in the presence of iron ($FeCl_3$) leads to increased ferritin synthesis, with desensitization to hydrogen peroxide resulting from a combination of lysosomal iron exocytosis and enrichment of lysosomes with ferritin via autophagocytosis. The accumulation of heavy metals into macrophage lysosomal compartments and lysosomal (iron) exocytosis are clearly well known processes that should now be examined in relation to Nramp1 expression/mutation. They are also processes that are of interest in relation to the hypothesis [31] that Nramp1 will be involved in macrophage-mediated recycling of iron from senescent red cells. Since Nramp2 and Nramp1 are both expressed in macrophages [32], iron recycling could involve an important interplay between Nramp1 and Nramp2 functions. Nramp2, for example, has two splice variants, one with a putative iron-responsive element in its 3′ untranslated region that confers iron-dependent mRNA stabilization [17] and another without this iron-responsive element [45]. It is unclear which of these is expressed in macrophages, and therefore whether the effect of Nramp1 on cytoplasmic iron levels will stabilize Nramp2 expression in the same way as has been demonstrated for other markers of macrophage activation [46].

Confirmation that Nramp1/NRAMP1 transports Fe^{2+}, Zn^{2+} and Mn^{2+} has many important implications for infectious [3,4] and autoimmune [5–7] disease associations, and the multiple pleiotropic effects (reviewed in [1,2]) associated with polymorphism in mouse and man. In the case of the regulation of arthritic diseases [5,7], NRAMP1 may contribute directly to the statistically significant increase in iron deposition observed in the synovial membrane of rheumatoid arthritis compared with osteoarthritis patients [47]. The inverse correlation between haemoglobin and erythrocytes in the serum and the amount of iron in the synovial membrane [47] also suggests a role in disease-associated anaemia. Indeed, polymorphism and the role of NRAMP1/2 should be examined more broadly in the context of both the anaemias of chronic disease, inflammatory, infectious or neoplastic disorders, and nutritionally related anaemias (reviewed in [48,49]). We have also recently demonstrated [50] that Nramp1 is expressed in neurons and affects behaviour and hypothalamus–pituitary–adrenal axis activation in response to stress. Defects in NRAMP1 may therefore also contribute to the inappropriate accumulation of metal ions observed in affected neurons in the substantia nigra in patients with Parkinson's [51–53] and other [54] neurodegenerative diseases.

The many cellular functions dependent on metal ions as cofactors goes some way to explaining the multiple pleiotropic effects of the Nramp1/NRAMP1 protein, and its complex role in both infectious and autoimmune disease susceptibility. They also broaden the context for possible disease associations in man. The strong sequence conservation of Nramp-family genes across eukaryotic and prokaryotic boundaries, and our demonstration that Nramp1/NRAMP1 function is mechanistically different from Nramp2/NRAMP2, prompts further analysis of the molecular structure, evolution and specialization of members of this important family of bivalent cation transporters.

This work was supported by the Wellcome Trust. T.G. holds a U.K. Medical Research Council research studentship.

REFERENCES

1 Blackwell, J. M. and Searle, S. (1999) Genetic regulation of macrophage activation: understanding the function of Nramp1 (= Ity/Lsh/Bcg). Immunol. Lett. **65**, 73–80
2 Blackwell, J. M., Searle, S., Goswami, T. and Miller, E. N. (2000) Understanding the multiple functions of Nramp1. Microbes Infect. **2**, 317–321

3 Bellamy, R., Ruwende, C., Corrah, T., McAdam, K. P. W. J., Whittle, H. C. and Hill, A. V. S. (1998) Variation in the NRAMP1 gene is associated with susceptibility to tuberculosis in West Africans. N. Engl. J. Med. **338**, 640–644

4 Abel, L., Sanchez, F. O., Oberti, J., Thuc, N. V., Hoa, L. V., Lap, V. D., Skamene, E., Lagrange, P. H. and Schurr, E. (1998) Susceptibility to leprosy is linked to the human NRAMP1 gene. J. Infect. Dis. **177**, 133–145

5 Shaw, M.-A., Clayton, D., Atkinson, S. E., Williams, H., Miller, N., Sibthorpe, D. and Blackwell, J. M. (1996) Linkage of rheumatoid arthritis to the candidate gene NRAMP1 on 2q35. J. Med. Genet. **33**, 672–677

6 Hofmeister, A., Neibergs, H. L., Pokorny, R. M. and Galanduik, S. (1997) The natural resistance-associated macrophage protein gene is associated with Crohn's disease. Surgery **122**, 173–179

7 Sanjeevi, C. B., Miller, E. N., Dabadghao, P., Rumba, I., Shtauvere, A., Denisova, A., Clayton, D. and Blackwell, J. M. (2000) Polymorphism at NRAMP1 and D2S1471 loci associated with juvenile rheumatoid arthritis. Arthritis Rheum. **43**, 1397–1404

8 Gruenheid, S., Pinner, E., Desjardins, M. and Gros, P. (1997) Natural resistance to infections with intracellular pathogens: The Nramp1 protein is recruited to the membrane of the phagosome. J. Exp. Med. **185**, 717–730

9 Searle, S., Bright, N. A., Roach, T. I. A., Atkinson, P. G. P., Barton, C. H., Meloen, R. H. and Blackwell, J. M. (1998) Localisation of Nramp1 in macrophages: modulation with activation and infection. J. Cell Sci. **111**, 2855–2866

10 Vidal, S. M., Malo, D., Vogan, K., Skamene, E. and Gros, P. (1993) Natural resistance to infection with intracellular parasites: isolation of a candidate for Bcg. Cell (Cambridge, Mass.) **73**, 469–485

11 Cellier, M., Belouchi, A. and Gros, P. (1996) Resistance to intracellular infections: Comparative genomic analysis of Nramp. Trends Genet. **12**, 201–204

12 Hughes, A. L. (1998) Protein phylogenies provide evidence of a radical discontinuity between arthropod and vertebrate immune systems. Immunogenetics **47**, 283–296

13 Supeck, F., Supekova, L., Nelson, H. and Nelson, N. (1996) A yeast manganese transporter related to the macrophage protein involved in conferring resistance to mycobacteria. Proc. Natl. Acad. Sci. U.S.A. **93**, 5105–5110

14 Orgad, S., Nelson, H., Segal, D. and Nelson, N. (1998) Metal ions suppress the abnormal taste behavior of the Drosophila mutant malvolio. J. Exp. Biol. **201**, 115–120

15 Rodrigues, V., Cheah, V. P. Y., Ray, K. and Chia, W. (1995) Malvolio, the Drosophila homologue of mouse Nramp1 (Bcg), is expressed in macrophages and in the nervous system and is required for normal taste behaviour. EMBO J. **14**, 3007–3020

16 Fleming, M. D., Trenor, C. C., Su, M. A., Foernzler, D., Beier, D. R., Dietrich, W. F. and Andrews, N. C. (1997) Microcytic anaemia mice have a mutation in Nramp2, a candidate iron transporter gene. Nat. Genet. **16**, 383–386

17 Gunshin, H., Mackenzie, B., Berger, U. V., Gunshin, Y., Romero, M. F., Boron, W. F., Nussberger, S., Gollan, J. L. and Hediger, M. A. (1997) Cloning and characterization of a mammalian proton-coupled metal-ion transporter. Nature (London) **388**, 482–488

18 Zwilling, B. S., Kuhn, D. E., Wikoff, L., Brown, D. and LaFuse, W. (1999) The role of iron in Nramp1 mediated inhibition of mycobacterial growth. Infect. Immun. **67**, 1386–1392

19 Aballay, A., Sarrouf, M. N., Colombo, M. I., Stahl, P. D. and Mayorga, L. S. (1995) Zn^{2+} depletion blocks endosome fusion. Biochem. J. **312**, 919–923

20 de Chastellier, C., Frehel, C., Offredo, C. and Skamene, E. (1993) Implication of phagosome-lysosome fusion in restriction of Mycobacterium avium growth in bone marrow macrophages from genetically resistant mice. Infect. Immun. **61**, 3775–3784

21 Hackam, D. J., Rotstein, O. D., Zhang, W., Gruenheid, S., Gros, P. and Grinstein, S. (1998) Host resistance to intracellular infection: mutation of natural resistance-associated macrophage protein 1 (Nramp1) impairs phagosomal acidification. J. Exp. Med. **188**, 351–364

22 Lang, T., Prina, E., Sibthorpe, D. and Blackwell, J. M. (1997) Nramp1 transfection transfers Ity/Lsh/Bcg-related pleiotropic effects on macrophage activation: Influence on antigen processing and presentation. Infect. Immun. **65**, 380–386

23 Barton, C. H., Whitehead, S. H. and Blackwell, J. M. (1995) Nramp transfection transfers Ity/Lsh/Bcg-related pleiotropic effects on macrophage activation: Influence on oxidative burst and nitric oxide pathways. Mol. Med. **1**, 267–279

24 Wall, D. A. and Patel, S. (1989) Isolation of plasma membrane complexes from Xenopus oocytes. J. Membr. Biol. **107**, 189–201

25 Liu, X. F. and Culotta, V. C. (1999) Post-translation control of Nramp metal transport in yeast. Role of metal ions and the BSD2 gene. J. Biol. Chem. **274**, 4863–4868

26 Liu, X. F. and Culotta, V. C. (1999) Mutational anlaysis of *Saccharomyces cerevisiae* Smf1p, a member of the Nramp family of metal transporters. J. Mol. Biol. **289**, 885–891

27 Jabado, N., Jankowski, A., Dougaparsad, S., Picard, V., Grinstein, S. and Gros, P. (2000) Natural resistance to intracellular infections: Natural resistance-associated macrophage protein 1 (NRAMP1) functions as a pH-dependent manganese transporter at the phagosomal membrane. J. Exp. Med. **192**, 1237–1247

28 Pinner, E., Gruenheid, S., Raymond, M. and Gros, P. (1997) Functional complementation of the yeast divalent cation transporter family SMF by NRAMP2, a member of the mammalian natural resistance-associated macrophage protein family. J. Biol. Chem. **272**, 28933–28938

29 Picard, V., Govoni, G., Jabado, N. and Gros, P. (2000) Nramp2 (DCT1/DMT1) expressed at the plasma membrane transports iron and other divalent cations into a calcein accessible cytoplasmic pool. J. Biol. Chem. **275**, 35738–35745

30 Canonne-Hergaux, F., Gruenheid, S., Ponka, P. and Gros, P. (1999) Cellular and subcellular localization of the nramp2 iron transporter in the intestinal brush border and regulation by dietary iron. Blood **93**, 4406–4417

31 Fleming, M. D., Romano, M. A., Su, M. A., Garrick, L. M., Garrick, M. D. and Andrews, N. C. (1998) Nramp2 is mutated in the anemic Belgrade (b) rat: evidence of a role for Nramp2 in endosomal iron transport. Proc. Natl. Acad. Sci. U.S.A. **95**, 1148–1153

32 Gruenheid, S., Canonne-Hergaux, F., Gauthier, S., Hackam, D. J., Grinstein, S. and Gros, P. (1999) The iron transport protein NRAMP2 is an integral membrane glycoprotein that colocalizes with transferrin in recycling endosomes. J. Exp. Med. **189**, 831–841

33 Nelson, N. (1999) Metal ion transporters and homeostasis. EMBO J. **18**, 4361–4371

34 Goswitz, V. C. and Brooker, R. J. (1995) Structural features of the uniporter/synporter/antiporter superfamily. Protein Sci. **4**, 534–537

35 Nelson, N. (1994) Energizing porters by proton-motive force. J. Exp. Biol. **196**, 7–13

36 Griffith, J. K., Baker, M. E., Rouch, D. A., Page, M. G., Skurray, R. A., Paulsen, I. T., Chater, K. F., Baldwin, S. A. and Henderson, P. J. (1992) Membrane transport proteins: implications of sequence comparisons. Curr. Opin. Cell Biol. **4**, 684–695

37 Marger, M. D. and Saier, Jr., M. H. (1993) A major superfamily of transmembrane facilitators that catalyse uniport, symport and antiport. Trends Biochem. Sci. **18**, 13–20

38 Varela, M. F. and Griffith, J. K. (1993) Nucleotide and deduced protein sequences of the class D tetracycline resistance determinant: relationship to other antimicrobial transport proteins. Antimicrob. Agents Chemother. **37**, 1253–1258

39 Atkinson, P. G. P. and Barton, C. H. (1998) Ectopic expression of Nramp1 in COS-1 cells modulates iron accumulation. FEBS Lett. **425**, 239–242

40 Kuhn, D. E., Baker, B. D., Lafuse, W. P. and Zwilling, B. S. (1999) Differential iron transport into phagosomes isolated from the RAW264.7 macrophage cell lines transfected with Nramp1Gly169 or Nramp1Asp169. J. Leukocyte Biol. **66**, 113–119

41 Gomas, M. S. and Appelberg, R. (1998) Evidence for a link between iron metabolism and Nramp1 gene mediated inhibition of mycobacterial growth. Immunology **95**, 165–172

42 Garner, B., Roberg, K. and Brunk, U. T. (1998) Endogenous ferritin protects cells with iron-laden lysosomes against oxidative stress. Free Radical Res. **29**, 103–114

43 Yuan, X. M., Brunk, U. T. and Olsson, A. G. (1995) Effects of iron- and hemoglobin-loaded human monocyte-derived macrophages on oxidation and uptake of LDL. Arterioscler. Thromb. Vasc. Biol. **15**, 1345–1351

44 Yuan, X. M., Anders, W. L., Olsson, A. G. and Brunk, U. T. (1996) Iron in human atheroma and LDL oxidation by macrophages following erythrophagocytosis. Atherosclerosis (Shannon, Irel.) **124**, 61–73

45 Lee, P. L., Gelbart, T., West, C., Halloran, C. and Beutler, E. (1998) The human Nramp2 gene: characterization of the gene structure, alternative splicing, promoter region and polymorphisms. Blood Cells, Mol. Dis. **24**, 199–215

46 Brown, D. H., LaFuse, W. P. and Zwilling, B. S. (1997) Stabilized expression of mRNA is associated with mycobacterial resistance controlled by Nramp1. Infect. Immun. **65**, 597–603

47 Fritz, P., Saal, J. G., Wicherek, C., Konig, A., Laschner, W. and Rautenstrauch, H. (1996) Quantitative photometrical assessment of iron deposits in synovial membranes in different joint diseases. Rheumatol. Int. **15**, 211–216

48 Yip, R. and Dallman, P. R. (1988) The roles of inflammation and iron deficiency as causes of anemia. Am. J. Clin. Nutr. **48**, 1295–1300

49 Krantz, S. B. (1994) Pathogenesis and treatment of the anemia of chronic disease. Am. J. Med. Sci. **307**, 353–359

50 Evans, C. A. W., Harbuz, M. S., Ostenfeld, T., Norrish, A. and Blackwell, J. M. (2001) Nramp1 is expressed in neurones and is associated with behavioural and immune responses to stress. Neurogenetics, in the press

51 Jellinger, K. A., Kienzl, E., Rumpelmaier, G., Paulus, W., Riederer, P., Stachelberger, H., Youdim, M. B. and Ben-Shachar, D. (1993) Iron and ferritin in substantia nigra in Parkinson's disease. Adv. Neurol. **60**, 267–272

52 Gerlach, M., Ben-Shachar, D., Riederer, P. and Youdim, M. B. (1994) Altered brain metabolism of iron as a cause of neurodegenerative diseases? J. Neurochem. **63**, 793–807

53 Hirsch, E. C. and Faucheux, B. A. (1998) Iron metabolism and Parkinson's disease. Mov. Disord. **13**, 39–45

54 Multhaup, G. (1997) Amyloid precursor protein, copper and Alzheimer's disease. Biomed. Pharmacother. **51**, 105–111

Received 17 October 2000/1 December 2000; accepted 2 January 2001